Elsevier Editorial System(tm) for Catalysis Today

Manuscript Draft

Manuscript Number: CATTOD-D-19-00564R1

Title: The influence of the catalyst on the CO formation during Catalytic Wet Peroxide Oxidation process

Article Type: SI: EAAOP6

Keywords: Carbon monoxide; Metal-free catalyst; Catalytic Wet Peroxide Oxidation; Fenton; Graphene; MAX phase

Corresponding Author: Dr. jaime carbajo, Ph. D.

Corresponding Author's Institution: Universidad Autónoma de Madrid

First Author: jaime carbajo, Ph. D.

Order of Authors: jaime carbajo, Ph. D.; Asunción Quintanilla; Alicia García Costa; Jesús González Julián; Manuel Belmonte; Pilar Miranzo; Maria Isabel Osendi Miranda; Jose Antonio Casas

Abstract: Herein, the formation of carbon monoxide as a harmful product upon the Catalytic Wet Peroxide Oxidation process is studied in presence of different solid catalysts: an iron supported activated carbon catalyst, a metal-free catalyst based on Graphene Nanoplatelets, and 1.6 wt. % Fe containing Cr2AlC MAX phase catalyst. The CWPO performance and the evolution of the gas effluent have been compared to that obtained in a conventional Fenton process.
Carbon monoxide yield released was significantly lower in Catalytic Wet Peroxide Oxidation process in relation to that obtained in the Fenton process, where CO concentration reaches a maximum of 6651 mg/Nm3. By contrast, in presence of activated carbon-Fe catalyst and, notably, Graphene Nanoplatelets and Cr2AlC MAX phase catalysts, a more progressive phenol and aromatics intermediates oxidation resulted in a much lower CO maximum concentration in the gas phase at the exit of the reactor of 2454 mg/Nm3, 170 mg/Nm3 and 187 mg/Nm3, respectively.
Hence, when compared to the homogeneous Fenton oxidation, Catalytic Wet Peroxide Oxidation process results be a more sustainable treatment for high-loaded phenolic wastewaters by decreasing the hazardous CO gaseous emissions avoiding this way a secondary pollution during the oxidation process.

Highlights

- *CO and CO_2 is monitored upon Catalytic Wet Peroxide Oxidation process and Fenton process*
- *CO formation was significantly lower in Catalytic Wet Peroxide Oxidation process than in Fenton*
- *CO selectivity is substantially affected by the catalyst nature*
- *Graphene Nanoplatelets and Cr_2AlC MAX catalysts were efficiently applied in Catalytic Wet Peroxide Oxidation*

*Graphical Abstract (for review)

Graphical Abstract

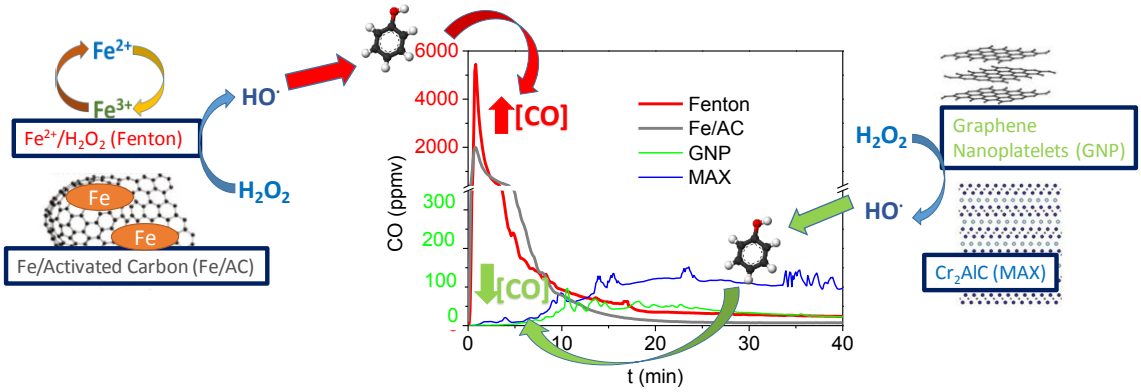

The influence of the catalyst on the CO formation during Catalytic Wet Peroxide Oxidation process

J. Carbajo[a]*, A. Quintanilla[a], A. L. Garcia-Costa[a], J. González-Julián[b], M. Belmonte[c], P. Miranzo,[c] M. I. Osendi[c], J. A. Casas[a]

[a]Chemical Engineering Department, Universidad Autonoma de Madrid, 28049 Madrid, Spain

[b]Forschungszentrum Jülich GmbH, Institute of Energy and Climate Research, Materials Synthesis and Processing (IEK-1), 52425 Jülich, Germany

[c]Institute of Ceramics and Glass (ICV-CSIC), Kelsen 5, 28049 Madrid, Spain

*Corresponding author. Tel: +34 914975599. E-mail address: jaime.carbajo@uam.es

Abstract

Herein, the formation of carbon monoxide as a harmful product upon the Catalytic Wet Peroxide Oxidation process is studied in presence of different solid catalysts: an iron supported activated carbon catalyst, a metal-free catalyst based on Graphene Nanoplatelets, and 1.6 wt. % Fe containing Cr_2AlC MAX phase catalyst. The CWPO performance and the evolution of the gas effluent have been compared to that obtained in a conventional Fenton process.

Carbon monoxide yield released was significantly lower in Catalytic Wet Peroxide Oxidation process in relation to that obtained in the Fenton process, where CO concentration reaches a maximum of 6651 mg/Nm^3. By contrast, in presence of *activated carbon-Fe* catalyst and, notably, *Graphene Nanoplatelets* and *Cr_2AlC MAX phase* catalysts, a more progressive phenol and aromatics intermediates oxidation

resulted in a much lower CO maximum concentration in the gas phase at the exit of the reactor of 2454 mg/Nm^3, 170 mg/Nm^3 and 187 mg/Nm^3, respectively.

Hence, when compared to the homogeneous Fenton oxidation, Catalytic Wet Peroxide Oxidation process results be a more sustainable treatment for high-loaded phenolic wastewaters by decreasing the hazardous CO gaseous emissions avoiding this way a secondary pollution during the oxidation process.

Keywords: Carbon monoxide, Metal-free catalyst, Catalytic Wet Peroxide Oxidation, Fenton, Graphene, MAX phase

1. Introduction

Nowadays, Advanced Oxidation Processes (AOPs) are considered efficient technologies for the treatment of wastewater with recalcitrant compounds [1-4]. In AOPs, *in situ* generated hydroxyl radicals (HO·) are the main responsible for abatement of pollutants through different by-products which can be eventually oxidized to CO_2 and H_2O [5]. Nevertheless, one of the main concerns regarding AOPs is the potential formation of harmful oxidation intermediates that, occasionally, can present even more toxicity than their parent pollutants [6-9].

Many works have focused on the possible formation of hazardous by-products in the liquid phase [9-11] but, unfortunately, the analysis of harmful products that can be released to the gas phase has not been conveniently addressed. In this sense, few studies dealing with air purification by photocatalytic oxidation have revealed that carbon monoxide is always present as a final oxidation product along with CO_2 [12-14]. Only recently Carbajo *et al.* have demonstrated that significant amounts of CO are also

produced during Fenton oxidation processes [15,16]. These works reflect the critical effect of the type of oxidizing pollutant and operational conditions on the carbon monoxide formation during the AOPs.

On the other hand, among all the AOPs technologies, Catalytic Wet Peroxide Oxidation (CWPO) emerges as an attractive alternative to the employment of dissolved Fe in the Fenton process. In this sense, heterogeneous catalysts can decompose H_2O_2 generating hydroxyl radicals (HO·) by a redox cycle. Additionally, these processes limit the generation of Fe sludge allowing to work in a wide range of pH, one of the main drawbacks of the Fenton process [17]. Over the last decades many works have been devoted to the study of iron-based materials (Heterogeneous Fenton), where iron is usually supported on activated carbons [17,18] , pillared clays [19], alumina [20] or zeolitic materials [21], among others. At present, the trend of CWPO processes is the search and the development of stable and efficient redox catalysts capable to avoid metal leaching [17,22]. In this regard, different works are focused on design of metal-free catalysts as promising alternatives to metal-based catalysts [23-26]. Graphene and graphene oxide (GO) are good examples of these new metal-free materials for the abatement of pollutants in water by the CWPO processes [22].

Herein, the efficiency of Catalytic Wet Peroxide Oxidation (CWPO) process with different catalysts has been studied, paying special attention to carbon monoxide production. These results have been compared to that obtained with the homogeneous Fenton process. Three catalysts with substantial differences have been selected: (i) a conventional metal-based catalyst based on Fe supported on Active carbon (Fe/AC), (ii) one metal-free catalysts with a 2-dimensional structure consisting on Graphene Nanoplatelets (GNP) and (iii) a Fe doped MAX phase based on Cr_2AlC.

The results of this work provide new valuable data regarding the importance of monitoring the gas phase generated during the treatment of high-loaded wastewaters, while, on the other hand, the appropriate selection of the catalysts can improve the environmental sustainability of the CWPO process, decreasing the secondary pollution caused by CO emissions during the oxidation process.

2. Materials and Methods

2.1 Catalysts preparation

Table 1 summarizes some characteristics of the catalysts employed in this work. Briefly, the iron supported activated carbon catalysts (Fe/AC) with a nominal iron content of 4% w/w was prepared by incipient impregnation at room temperature with an aqueous solution of iron nitrate in a commercial activated carbon, supplied by Merck (Cod. 102514; d_p: 1.5 mm). The sample was dried 12 h at 70 ºC and finally, heat treated at 200 ºC in air atmosphere for 4 h. As can be seen in Table 1, this catalyst presented a high surface area, around 930 m^2/g, and relatively high concentration of oxygenated surface groups due to the final heat-treatment in air atmosphere. More preparation details are provided elsewhere [27].

Graphene nanoplatelets (GNP), obtained from Angstron Materials Inc., was employed as received in powder form. GNP presented a through-plane dimension of 50-100 nm (see Figure 1), a low oxygen content (less than 2 %) and a relatively low S_{BET} (≤ 40 m^2/g) (Table 1). Content of oxygen was quantified by elemental analysis in a LECO Model CHNS-932 analyser. GNP nanopowder was also characterized by thermogravimetric analysis (TGA, SDT Q600, TA Instruments) carried out in air from room temperature to 1000 °C at a heating rate of 3 °C·min^{-1}. Total reflection X-Ray

Fluorescence (TXRF) was performed in a TXRF S2 PicoFox, (Bruker) to determine the metal content in the GNP catalyst, thus Fe content was below 0.02 % (see Table 1).

Cr_2AlC MAX powder was synthesized from the reaction of their elemental constituents (chromium, aluminium and graphite) at high temperature (1350 ºC) in argon atmosphere, according to the procedure described elsewhere [28]. The compacted MAX specimen was planetary milled with zirconia balls to achieve a mean particle size of 0.9 µm (see Figure 1). The powder, with a S_{BET} value of 10 m^2/g, had a purity of 97.1%, determined by inductively coupled plasma-optical emission spectroscopy (ICP-OES), and contained a 1.6 wt.% of Fe that came from the raw chromium constituent and 1.2 wt.%. of oxygen. X-Ray diffraction (XRD) patters of MAX was performed in a D8 Advance diffractometer, Bruker (see Figure S4). XRD pattern was consistent to a bulk ordered Cr_2AlC MAX phase with a less intense Al_2O_3 phase attributable to oxide surface layer.

2.2 CWPO experiments

CWPO experiments were carried out in a high-pressure reactor (BR-300, BERGHOF) which operated in a discontinuous mode for the liquid phase but in continuous mode for the gas. In order to analyse the gas composition during the process, 1 L/min N_2 stream was continuously introduced into the reactor. The gas effluent generated along the oxidation process was conducted to a CO and CO_2 detector. Further details are given elsewhere [15,16].

The selected operating conditions in all trials were: 1000 mg/L of initial phenol concentration, the stoichiometric amount of hydrogen peroxide for complete mineralization (5000 mg/L), T = 80 ºC, atmospheric pressure and 5 g/L of catalyst in CWPO experiments or 100 mg/L of Fe^{2+} in the Fenton trials. An initial pH_0 of 3 was selected in order to compare the results. Briefly, 300 mL of a solution containing 1000

mg/L of phenol and the appropriate amount of catalyst were introduced in the reactor and the solution was heated up to 80 ºC. At this point, the stoichiometric amount of H_2O_2 was injected, considering this step the beginning of the reaction.

2.3 Analytical methods

Liquid samples from the reactor were analysed at different reaction times. Phenol and aromatic by-products were quantified by high performance liquid chromatography (Thermo Fisher Scientific) using a C18 column (Eclipse Plus C18, 150 x 4.6 mm, 5 μm) at 323 K with a 4 mM aqueous sulfuric acid solution at 1 $mL \cdot min^{-1}$ as mobile phase. Short-chain organic acids were analysed by ion chromatography (IC) equipped with a conductivity detector (Metrohm 883 IC) using a Metrosep A supp 5 column (250 x 4 mm) and 0.7 $mL \cdot min^{-1}$ of an aqueous solution of 3.2 mM Na_2CO_3 and 1 mM $NaHCO_3$ as the mobile phase. Total organic carbon (TOC) in solution was measured using a TOC analyser (Shimadzu, mod. TOC-Vsch). H_2O_2 concentration was determined by colorimetric $TiOSO_4$ method using a UV2100 Shimadzu UV–vis spectrophotometer.

CO and CO_2 were continuously monitored using an Ultramat 23 infrared detector (Siemens). CO_2 and CO signals in ppmv were recorded every 6 s. The accumulated amounts of CO_2 and CO (in mg) along the oxidation processes were calculated by integration of concentration profiles. A second-order kinetic equation has been selected to fit the time evolution of TOC in phenol oxidation with Fenton and CWPO processes. For its part, the initial rate of CO_2 formation calculated by the linearization of CO_2 kinetic curve for the initial 15 min has been also included.

3. Results and discussion

3.1 CWPO performance

The concentration of TOC, phenol, aromatics, acids and the accumulated amount of CO and CO_2 for the CWPO with Fe/AC, GNP and MAX catalysts have been represented in Figure 2 and 3, respectively, and, as can be seen, significantly different behaviours can be observed in all the studied solid catalysts. For the sake of comparison, the results obtained in a conventional Fenton process have been also collected in Figure 2.

Interestingly, although TOC elimination with the Fe/AC catalyst was noticeably higher than in the homogeneous Fenton process, CO_2 and CO evolved to a much lesser extent (see Figure 2). As can be seen, this is consistent with the kinetic parameters provided in Table 2, where the apparent kinetic constant for TOC disappearance for Fe/AC was much higher compared to the homogeneous Fenton process while, on the contrary, the calculated CO_2 production rate was substantially lower. In this sense, as can be seen in the carbon mass balance, represented in Figure 4, a great imbalance (~55 %) between the TOC removed from the liquid phase and the CO/CO_2 produced is observed in the Fe/AC catalyst. This imbalance is directly attributable to the strong adsorption of different by-products on the actived carbon surface. Thus, when Fe/AC catalyst was employed, fast decomposition of H_2O_2 (see Figure S1 of the Supporting Information) provokes a high concentration of HO· in the initial stage of the reaction favoring the formation of organic radicals and condensation by-products [29,30], these species remain adsorbed in a large extent on the solid surface (see Figure 4). Additionally, the abrupt end of the oxidation process with Fe/AC coincided with the complete H_2O_2 consumption, which occurred at approximately 20-30 min (see Figure S1). Hence, although an 85 % of TOC disappearance was achieved with Fe/AC catalyst, only 30 % of the initial TOC was actually mineralized to CO_2. In this sense, the relatively high content of oxygen in Fe/AC catalyst (see Table 1) is attributable to the presence surface oxygen groups (SOGs). These SOGs can act as anchorage sites and promote the

dispersion of Fe particles, which catalytically decompose hydrogen peroxide into HO·. Nevertheless, TOC removal in Fe/AC can be limited to a certain extent by this SOGs, species that have been also related to the inefficient H_2O_2 decomposition to non reactive O_2 instead of to HO· radical [31].

As can be seen in Figure 3 and Table 2, lower TOC and phenol degradation rates were attained for the CWPO with GNP and MAX catalysts. Nonetheless, X_{TOC} for GNP and MAX catalysts was 45.9 and 53.8 % at 80 min of reaction time, respectively. Besides, the carbon mass balance for GNP and MAX catalysts (Figure 4) shows that, at the end the process, the TOC removed from the liquid phase fits in a large extent to the produced CO_2, then, compared to Fe/AC, a much lower fraction of by-products adsorbed on the surface of the MAX, and notably, GNP catalyst is evidenced. Thus, practically all the eliminated TOC using both catalysts was efficiently mineralized to CO/CO_2 along the process. Additionally, GNP and MAX catalysts show a more efficient use of H_2O_2 (see Fig. S1), whose decomposition must be occurring through the formation of HO· at a lower rate, thus limiting the organic radicals formation and the generation of condensation products.

The promising mineralization results and more efficient decomposition of H_2O_2 to HO· with GNP catalysts, particularly taking into account its metal-free nature, has been attributed to the presence of structural defects, such as quinone and pyrone structures, usually considered active sites for H_2O_2 decomposition to produced HO· in graphene-based materials [32]. Additionally, GNP efficiency has been also related in a previous work [22] to a lower content of oxygenated groups compared to other graphene-based materials, such as graphene oxide. In this regard, accordingly to surface characterization carried out by ATR-FTIR analysis [22], the GNP catalysts did not presented high

contents of carboxylic, alcohol or ester groups, considered electron-withdrawing groups which can limited the electronic mobility.

For its part, the good catalytic behavior found in CWPO with MAX phase, certainly closed to that obtained in the Fenton homogeneous process, may be related in accordance to other authors [33] to a combination of numerous defects and the thin surface oxide layer rich in oxygen vacancies that makes MAX phases active heterogeneous catalysts. More likely, in the CWPO with MAX catalyst, consistent to a bulk ordered Cr_2AlC MAX phase (Fig S4, Supporting Information), a fundamental role must be played by the activation of hydrogen peroxide by the 1.6 wt. of Fe content (see Table 1) and Cr, which may play an additional role in the Fenton-like Cr/H_2O_2 oxidative system [34,35].

3.2 CWPO catalysts stability

In order to analyze in more detail the CWPO catalysts stability, the metal leaching with MAX and Fe/AC catalysts was determined. Thus, after 80 min of reaction time, 28 ppm of Fe were detected in the liquid phase when Fe/AC catalyst was employed, while 3.1 ppm of Cr, 12.7 ppm of Al and 7.8 ppm of Fe were found with MAX catalyst. For its part, no metal lixiviation was observed with GNP catalyst due to its metal-free character, in fact, the absence of metals in this catalyst was confirmed by TXRF (see Table 1) and TGA analysis where, as can be seen in Fig S3 (Supporting Information), weight loss come practically to 100 % at 800 ºC.

To test the reusability of the CWPO systems, all the catalysts were recovered by filtration and reused in a consecutive run in the same conditions. The results are depicted in Figure 5, where TOC and H_2O_2 conversions and X_{TOC}/X_{H2O2} ratios after two consecutive cycles are represented. Although Fe and Cr leaching can contribute to some extent to the homogenous Fenton-like process when MAX catalyst was employed, Fe

lixiviation significantly decreased in the second cycle (from 7.8 ppm to 4.2 ppm) whereas no substantial change in the TOC removal was observed (Figure 5). In this case, the bulk character of the Cr_2AlC phase (see Fig. S5) can explain the stability of this catalyst.

On the contrary, Fe lixiviation was certainly high when Fe/AC catalyst was used (28 ppm) and this lixiviation was maintained in large extent after a second cycle (22 ppm). In this case, the lower percentage of TOC removal after reuse can be attributed to the loss of the active iron phase by leaching and to the organic matter adsorption accumulated on the catalyst surface, which additionally can cause fouling in the metallic Fe particles on the carbon surface. Thus, Fe/AC reusability was particularly compromised by the low Fe anchorage stability and the decrease of the activated carbon adsorption capacity. For its part, as can be seen in Figure 5, TOC conversion was maintained fairly stable when GNP catalyst was re-used in a second cycle.

Efficient consumption of H_2O_2 is a critical issue of CWPO and Fenton processes since this is, by far, the main operating cost. For this reason, the amount of TOC converted per amount of H_2O_2 consumed, defined here by X_{TOC}/X_{H2O2} ratio, has been represented in Figure 5 at the end of each cycle. As can been seen, H_2O_2 consumption efficiency was significantly higher for the heterogeneous CWPO process (0.80-0.85) compared to that obtained in the homogeneous Fenton process (0.64). This can be attributed to an excess of hydroxyl radicals formation at the initial stages in the Fenton oxidation, which favours competitive reactions between radicals instead of reacting with organic matter [30], thereby leading to an inefficient H_2O_2 consumption and increasing the operational costs of Fenton process. Interestingly, although X_{TOC}/X_{H2O2} were substantially maintained in a second cycle for GNP and MAX catalysts, a significant decrease of this ratio was found in the Fe/AC (from 0.85 to 0.71). This evolution can be explained by an

important reduction of the activated carbon adsorption capacity in a second run, thus confirming that activated carbon can promote to a certain extent the inefficient decomposition of H_2O_2 into O_2 and H_2O.

3.3 Carbon monoxide selectivity

In order to gain an insight into the role of the catalyst nature on the CO selectivity during the CWPO, temporal profiles of the accumulated amount of CO and CO_2 are represented in Figure 6. Briefly, it can be noted that in Fenton and CWPO with Fe/AC, CO was rapidly produced at the beginning of the reaction due to the fast removal of phenol and aromatic species (see Figure 2), which is the main step involved in CO production [15]. On the contrary, lower degradation rates for phenol and aromatics took place with MAX and, notably, GNP catalysts. In both cases, CO production was low at the beginning of the reaction and a continuous progressive release of CO can be observed.

Interestingly, CO selectivity, expressed in Figure 7 as the amount in mg of CO in gas phase per mg of carbon dioxide produced, was significantly lower in CWPO compared to Fenton process. Likewise, CO selectivity seem to be substantially affected by the catalyst nature (i.e.: metallic based materials, metal free, catalyst supports properties…) employed in CWPO, thus demonstrating that different oxidation pathways or mechanisms in the catalyst surface can inhibit or favor the formation of CO. Despite the CO selectivity observed in the Fe/AC is initially comparable to that of the homogeneous Fenton (see Figure 7), CO selectivity evolved differently and was significantly reduced as long as the oxidation process progressed. Probably, the last is explained by strong aromatics and condensation by-products adsorption produced on the carbonaceous surface in the Fe/AC catalyst [27]. On the other hand, a different oxidation pathway could explain the lower selectivity found in MAX catalyst. In this sense, while phenol

oxidation with GNP and Fe/AC proceed mainly through hydroquinone and p-benzoquinone, as typically occurs in carbon-based catalysts [27,29] , MAX catalyst exhibited a predominant selectivity to catechol (see Figure S2 of the Supporting Info) being the latter less selective to CO in accordance with our previous work [15].

3.4 Analysis of CO and CO_2 concentrations in the gas effluent

The on-line concentration of CO and CO_2 in the gas emissions has been represented in Figure 8 for the homogeneous Fenton oxidation and for the CWPO process with Fe/AC, GNP and MAX, respectively. As can be seen in the Fenton process and in the CWPO with Fe/AC catalysts, fast ring opening of aromatics intermediates occurred at the initial stages of the reaction and CO release mainly took place at short reaction times (< 5 min). Hence, CO concentration reach a maximum of ca. 5450 ppmv (6720 mg/Nm^3) and 1990 ppmv (2454 mg/Nm^3) for Fenton and Fe/AC catalyst, respectively. By contrast, in presence of MAX catalyst, and notably, GNP catalyst, a significantly lower oxidation rate and a progressive phenol and aromatics intermediates oxidation resulted in a much lower CO maximum concentration released to the gas phase. Hence, CO concentration reached a maximum of 152 ppmv (187 mg/Nm^3) and 138 ppmv (170 mg/Nm^3) for MAX and GNP, respectively.

According to these results, the CO maximum emission values was in the case of the Fenton process 2.7, 39.5 and 35.4 times higher than those obtained with Fe/AC, GNP and MAX phase catalyst, respectively. Therefore, although a slightly lower degree of mineralization was achieved as expected in the CWPO process, these heterogeneous systems are capable to, on the one hand, maintain good TOC removal and H_2O_2 consumption efficiencies while, on the other, result in a minimization of CO production resulting in a substantial decrease of the hazardous gaseous emissions.

4. Conclusion

This work highlights the noticeable concentrations of CO that can be emitted in the gas phase generated during the treatment of high-loaded wastewaters by advanced oxidation treatments such as CWPO. The formation of CO during the CWPO of phenol with different solid catalysts have been studied, and the following conclusions can be drawn: Although CWPO process with graphene nanoplatelets and Cr_2AlC catalysts presented lower H_2O_2 conversions and TOC degradation rates, both catalysts maintained high mineralization efficiencies (X_{TOC}/X_{H2O2}) and low CO productions. CO selectivity in CWPO seem to be substantially affected by the catalyst nature (active phase, catalyst support properties…) employed. Thus, predominant selectivity to catechol in phenol oxidation explains the lower selectivity to CO found in MAX catalyst in comparison with GNP or Fe/AC. Lastly, the significantly high CO concentration emitted in the Fenton process (6720 mg/Nm^3) was notably reduced in presence of GNP (187 mg/Nm^3) and MAX (170 mg/Nm^3) catalysts, respectively.

This work proves that CWPO process with GNP and MAX catalysts, though require longer reaction times than Fenton to achieve similar oxidation degrees, consumed more efficiently H_2O_2, are less selective to CO and can significantly limit carbon monoxide concentrations released upon the treatment of high-loaded polluted wastewaters. Hence, when compared to homogeneous Fenton, CWPO results in a better sustainability decreasing the hazardous gaseous emissions and the secondary pollution found during the oxidation process.

Acknowledgments

This work was supported by the following project: CTM2016-76454-R and MAT2015-67437-R (Ministerio de Economía y Competititivad, MINECO). J. Carbajo wants to thank the Ministerio de Ciencia, Innovación y Universidades (MICIU) for a grant under the Juan de la Cierva_Incorporación programme (IJCI-2017-32682).

References

[1] A. R. Ribeiro, O.C. Nunes, M.F.R. Pereira, A.M.T. Silva, Environ. Int. 75 (2015) 33

[2] I. Oller, S. Malato, J.A. Sánchez-Pérez, Sci. Total. Environ. 409 (2011) 4141

[3] J. Carbajo, A. Bahamonde, M. Faraldos, Mol. Catal. 434 (2017) 167

[4] C. Amor, L. Marchão, M. S. Lucas, J. A. Peres, Water 11 (2019) 205

[5] S. Garcia-Segura, E. Brillas, Appl. Catal B: Environ 181 (2016) 681

[6] A. Sharma, J. Ahmad, S. J. S.Flora, Environ. Res. 167 (2018) 223

[7] J. Long, W. Wang, L. J. Xu, Crit. Rev. Env. Sci. Tec., 42 (2012) 251

[8] A.R. Fernández-Alba, D. Hernando, A. Agüera, J. Cáceres, S. Malato, Water Res., 36 (2002) 4255

[9] J. K. Kim, K. Choi, I. H. Cho, H. S. Son, K. D. Zoh, J. Hazard. Mater., 148 (2007) 281

[10] D. Syam Babu, V. Srivastava, P. V. Nidheesh, M. Suresh Kumar, Sci. Total. Environ. 696 (2019) 133961

[11] I. A. Ike, T. Karanfil, J. Cho, J. Hur, Water Res., 164 (2019) 114929

[12] D.S. Selishchev, N.S. Kolobov, A.A. Pershin, D.V. Kozlov, Appl. Catal. B: Environ., 200 (2017) 503

[13] D. S. Selishchev, P. A. Kolinko, D. V. Kozlov, J. Photochem. Photobiol. A: Chem. 229 (2012) 11

[14] N. S. Kovalevskiy, M. N. Lyulyukin, D. S. Selishchev, D. V. Kozlov, J. Hazard. Mat. 358 (2018) 302

[15] J. Carbajo, A. Quintanilla, J. A. Casas, Appl. Catal. B: Environ. 232 (2018) 55

[16] J. Carbajo, A. Quintanilla, J. A. Casas, Sep. Purif. Technol., 221 (2019) 269

[17] J. J. Rueda Márquez, I. Levchuk, M. Sillanpää, Catalysts 8 (2018) 673

[18] A. Rey, J.A. Zazo, J.A. Casas, A. Bahamonde, J. J. Rodriguez, Appl. Catal. A: Gen. 402 (2011) 146

[19] N. R. Sanabria, Y. M. Peralta, M. K. Montañez, N. Rodríguez-Valencia, R. Molina, S. Moreno, Water Sci. Technol. 66 (2012) 1663

[20] M. Munoz, F. J. Mora, Z. M. de Pedro, S. Alvarez-Torrellas, J. A. Casas, J. J. Rodriguez, J. Hazard. Mater 331 (2017) 45.

[21] G. Calleja, J. A. Melero, F. Martínez, R. Molina, Water Res. 39 (2005) 1741

[22] A. Quintanilla, J. Carbajo, J. A. Casas, P. Miranzo, M. I. Osendi, M. Belmonte, Catal. Today, (2019) In Press, https://doi.org/10.1016/ j.cattod.2019.06.026

[23] M. Pedrosa, G. Drazic, P. B. Tavares, J. L. Figueiredo, A. M. T. Silva, Chem. Eng. J., 369 (2019) 223

[24] D. Liu, L. Dai, X. Lin, J. F. Chen, J. Zhang, X. Feng, K. Müllen, X. Zhu, S. Dai Adv. Mater. 31(2019) 1804863

[25] M., Monaia, M. Melchionna, P. Fornasiero, Adv. Catal. 63 (2018) 1

[26] Y. Cui, Z. Ding, P. Liu, M. Antonietti, X. Fu, X. Wang, Phys. Chem. Chem. Phys. 14 (2012) 1455.

[27] A. Rey, M. Faraldos, J. A. Casas, J. A. Zazo, A. Bahamonde, J. J. Rodríguez, Appl. Catal. B: Environ 86 (2009) 69

[28] J. Gonzalez-Julian, S. Onrubia, M. Bram, O. Guillon, J. Ceram. Soc. Jpn. 124 (2016) 415

[29] J. A. Zazo, J. A. Casas, C. B. Molina, A. Quintanilla, J. J. Rodríguez, Environ. Sci. Technol. 41 (2007) 7164.

[30] J. A. Zazo, J. A. Casas, A. F. Mohedano, M. A. Gilarranz, J. J. Rodríguez, Environ. Sci. Technol. 39 (2005) 9295.

[31] A. Rey, M. Faraldos, A. Bahamonde, J. A. Casas, J. A. Zazo, J. J. Rodríguez, Ind. Eng. Chem. Res., 47 (2008) 8166

[32] J. C. Espinosa, J. C. Espinosa, S. Navalón, A. Primo, M. Moral, J. Fernández Sanz, M. Álvaro, H. García, Chem. Eur. J. 21 (2015) 11966

[33] W. H. K. Ng, E. S. Gnanakumar, E. Batyrev, S. K. Sharma, P. K. Pujari, H. F. Greer, W. Zhou, R. Sakidja, G. Rothenberg, M. W. Barsoum, N. Raveendran Shiju Angew. Chem. Int Ed. 57 (2018) 1

[34] A. D. Bokare, W. Choi, J. Hazard. Mat. 275 (2014) 121

[35] A. D. Bokare, W. Choi, Environ. Sci. Technol. 44 (2010) 7232

Table

Table 1. *Main CWPO catalysts properties.*

Catalyst	*Composition*	*Dimensions (nm)*	*S_{BET} (m^2/g)*	*Oxygen Content. (wt.%)*	*Fe (wt.%)*	*Supplier*
Fe/AC	*Fe supported on activated carbon*	*1500 nm*	*930*	*12.6*	*4.2*	*Homemade*
GNP	*Graphene Nanoplatelets*	*7000 x (50-100)*	*≤ 40*	*1.8*	*≤ 0.02**	*Angstrom Materials Inc.*
MAX	*MAX phase (Cr_2AlC)*	*≈1000*	*10*	*1.2*	*1.6*	*Homemade*

* Below the limit of detection, analysed by Total reflection X-ray fluorescence spectroscopy

Table 2. *Kinetic constant values based on TOC disappearance and initial rate of CO_2 formation.*

Catalyst	***k_{TOC} L/(mg· min)***	***r^2***	***r_{CO2} mg/min***	***r^2***
Fenton	*7.1×10^{-5}*	*0.98*	*40.3*	*0.98*
Fe/AC	*4.1×10^{-4}*	*0.96*	*19.8*	*0.99*
GNP	*1.5×10^{-5}*	*0.98*	*2.9*	*0.98*
MAX	*2.1×10^{-5}*	*0.96*	*3.9*	*0.97*

Figure

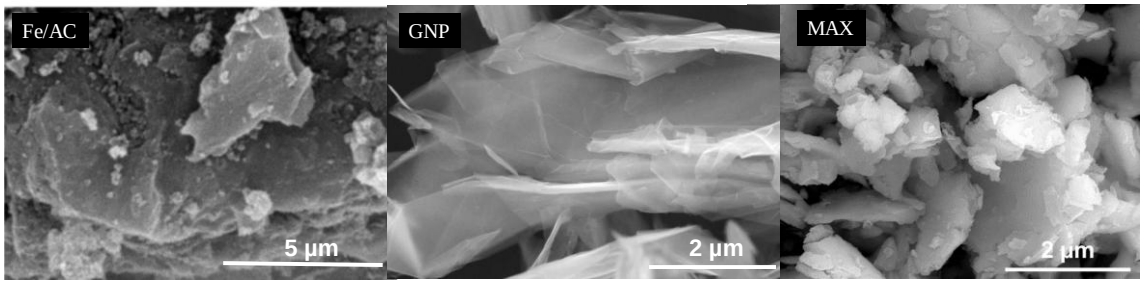

Fig. 1. SEM micrographs for Fe/AC, GNP and MAX catalysts

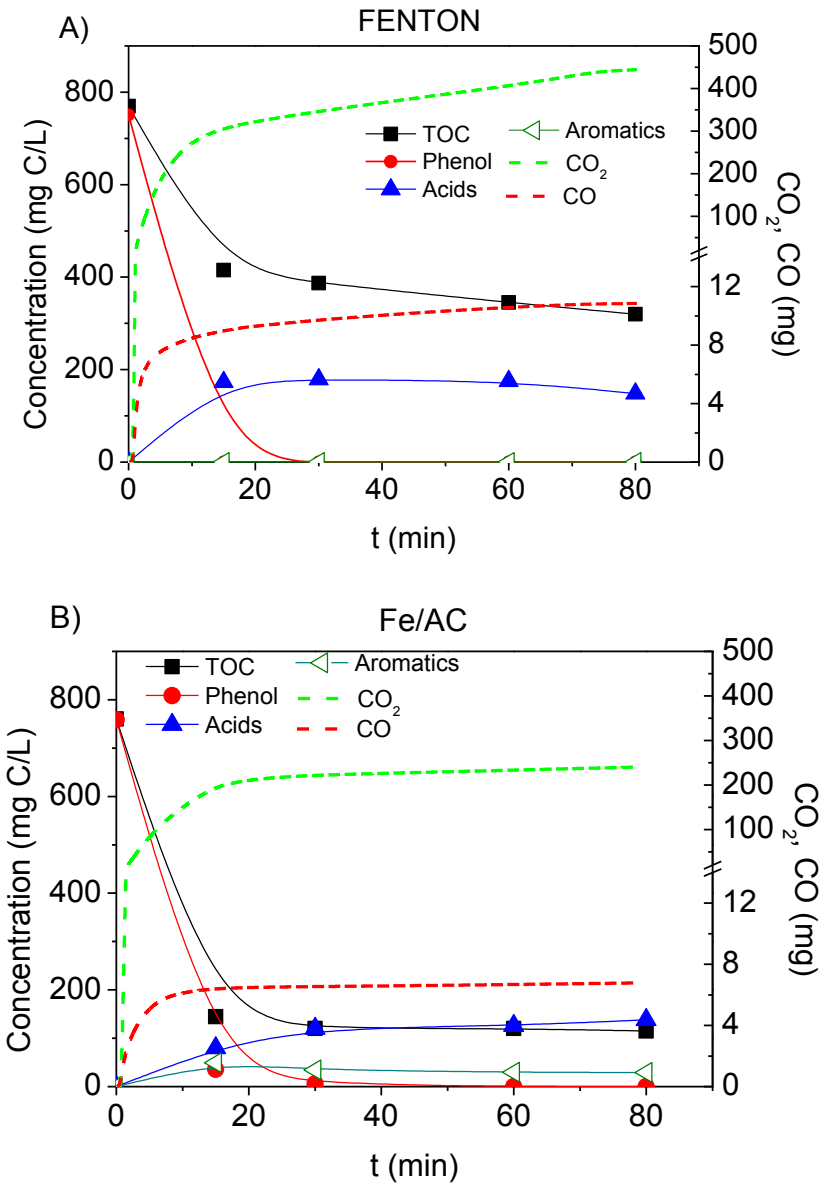

Figure 2. Evolution of Phenol, TOC, aromatics, acids and the accumulated amounts of CO and CO_2 emissions for Fenton oxidation (A) and CWPO with the Fe/AC catalysts (B).

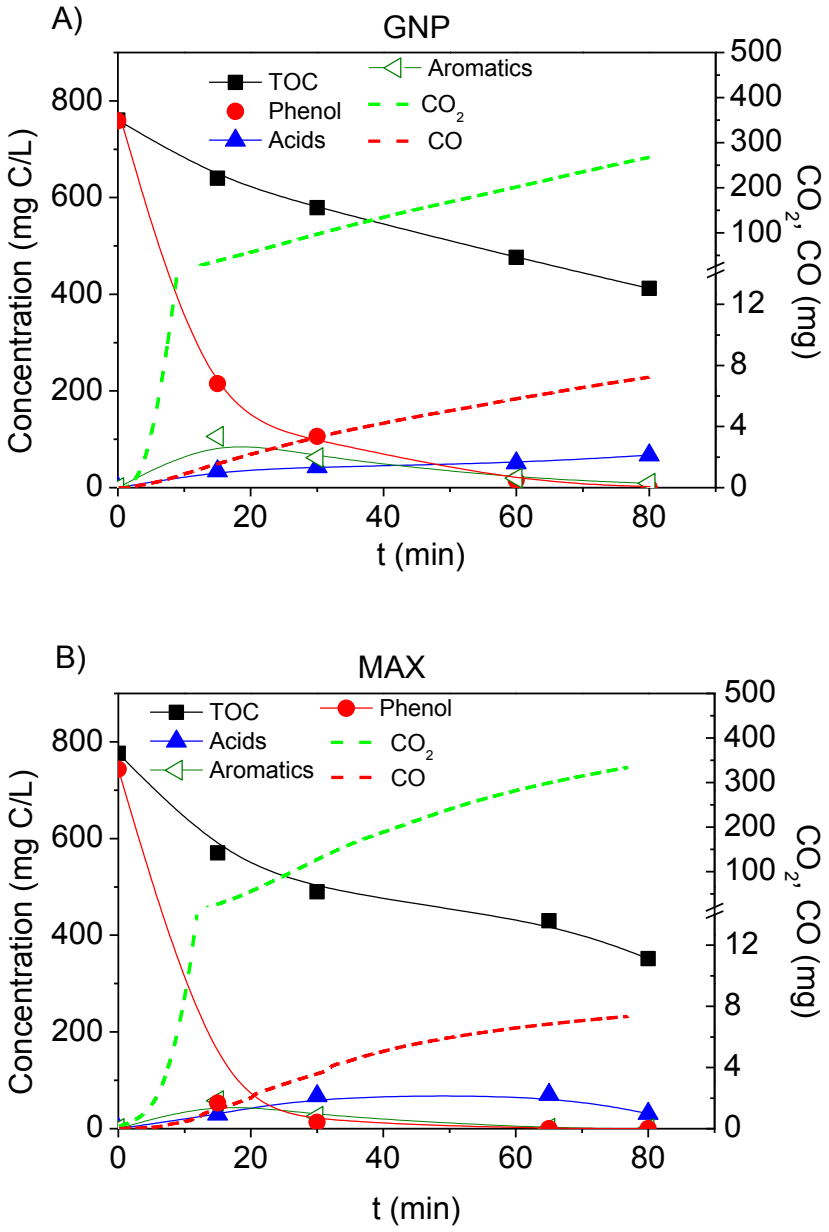

Figure 3. Evolution of Phenol, TOC, aromatics, acids and the accumulated amounts of CO and CO_2 emissions for the CWPO with the GNP (A) and MAX catalysts (B).

.

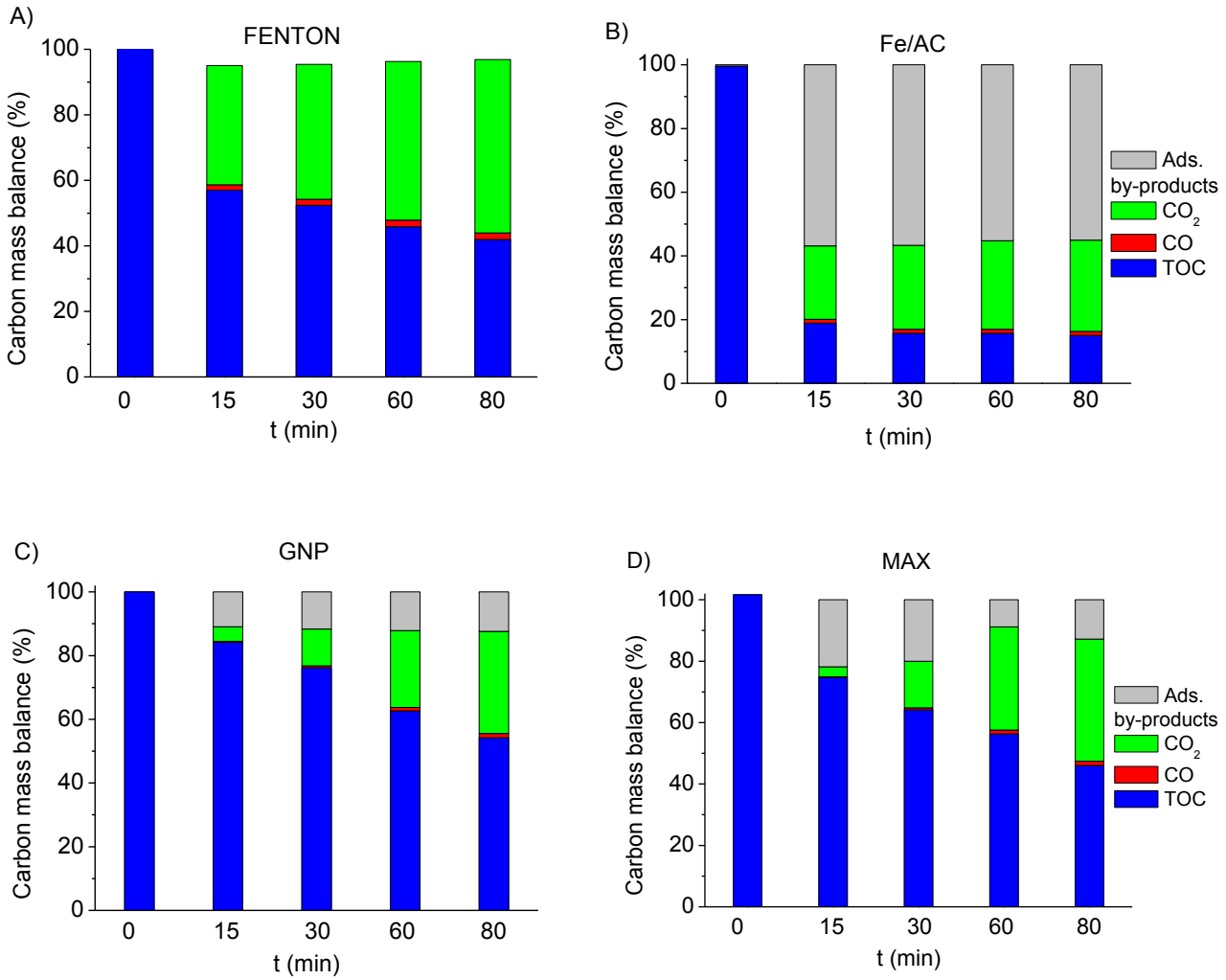

Figure 4. Carbon mass balance on the Fenton oxidation (A) and CWPO with Fe/AC (B), GNP (C) and MAX (D) catalysts.

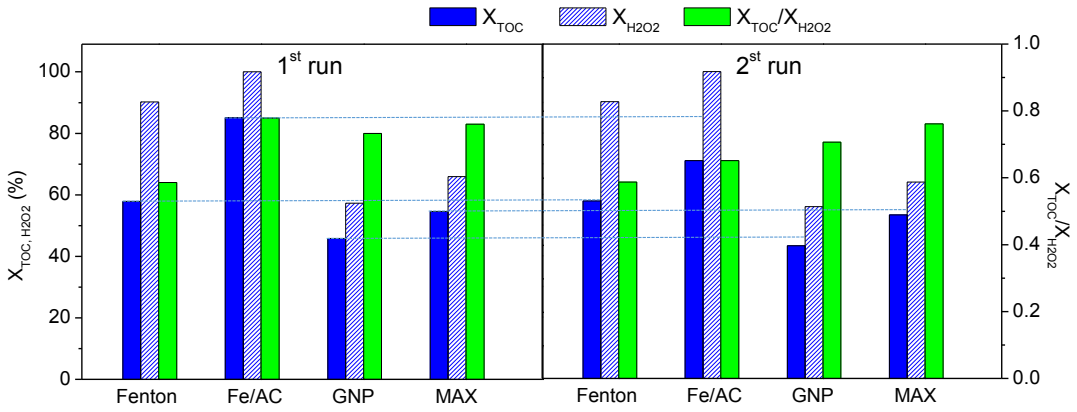

Figure 5. TOC and H_2O_2 conversions and X_{TOC}/X_{H2O2} ratios after 80min of reaction time for two consecutive runs for Fenton and CWPO with Fe/AC, GNP and MAX catalysts.

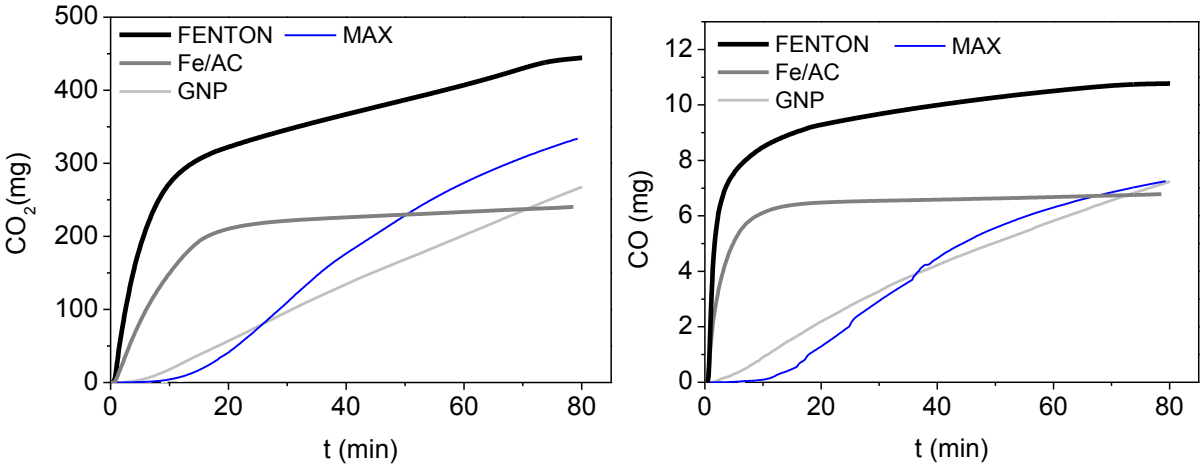

Figure 6. Temporal profiles of the accumulated amount of CO_2 (left) and CO (right) in mg produced in CWPO and Fenton oxidation processes.

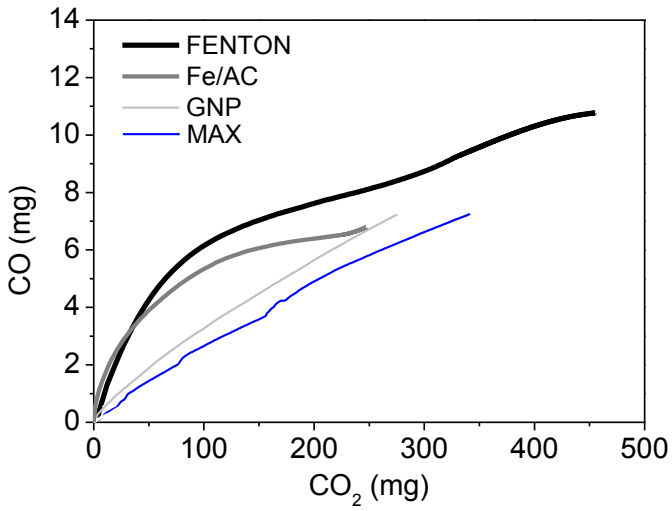

Figure 7. Evolution of the CO selectivity, expressed as the mg of CO in gas phase per mg of carbon dioxide produced, in CWPO and Fenton oxidation processes

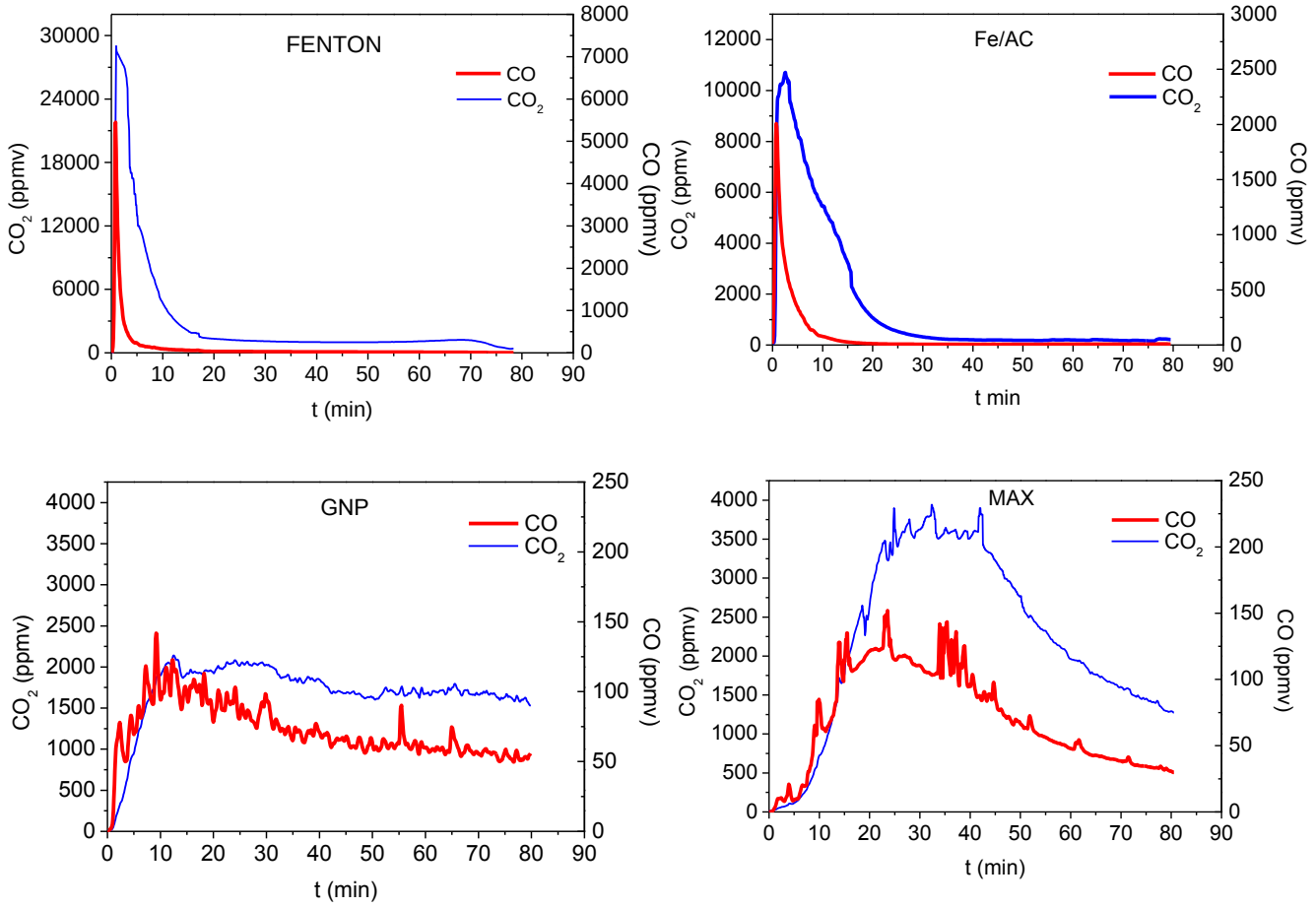

Figure 8. Continuous evolution of CO and CO_2 concentration in Fenton process and CWPO process with Fe/AC, GNP and MAX catalysts.

The influence of the catalyst on the CO formation during Catalytic Wet Peroxide Oxidation Process

J. Carbajo[a]*, A. Quintanilla[a], A. L. Garcia-Costa[a], J. González-Julián[b], M. Belmonte[c], P. Miranzo,[c] M. I. Osendi[c], J. A. Casas[a]

[a]Chemical Engineering Department, Universidad Autonoma de Madrid, 28049 Madrid, Spain

[b]Forschungszentrum Jülich GmbH, Institute of Energy and Climate Research, Materials Synthesis and Processing (IEK-1), 52425 Jülich, Germany

[c]Institute of Ceramics and Glass (ICV-CSIC), Kelsen 5, 28049 Madrid, Spain

*Corresponding author. Tel: +34 914975599. E-mail address: jaime.carbajo@uam.es

Supporting Information

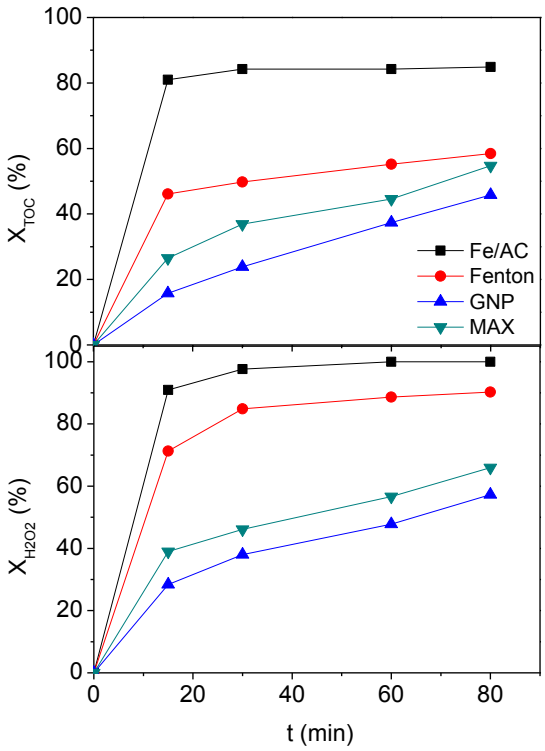

Figure S1. X_{TOC} and X_{H2O2} for Fenton process and CWPO with Fe/AC, GNP and MAX catalysts

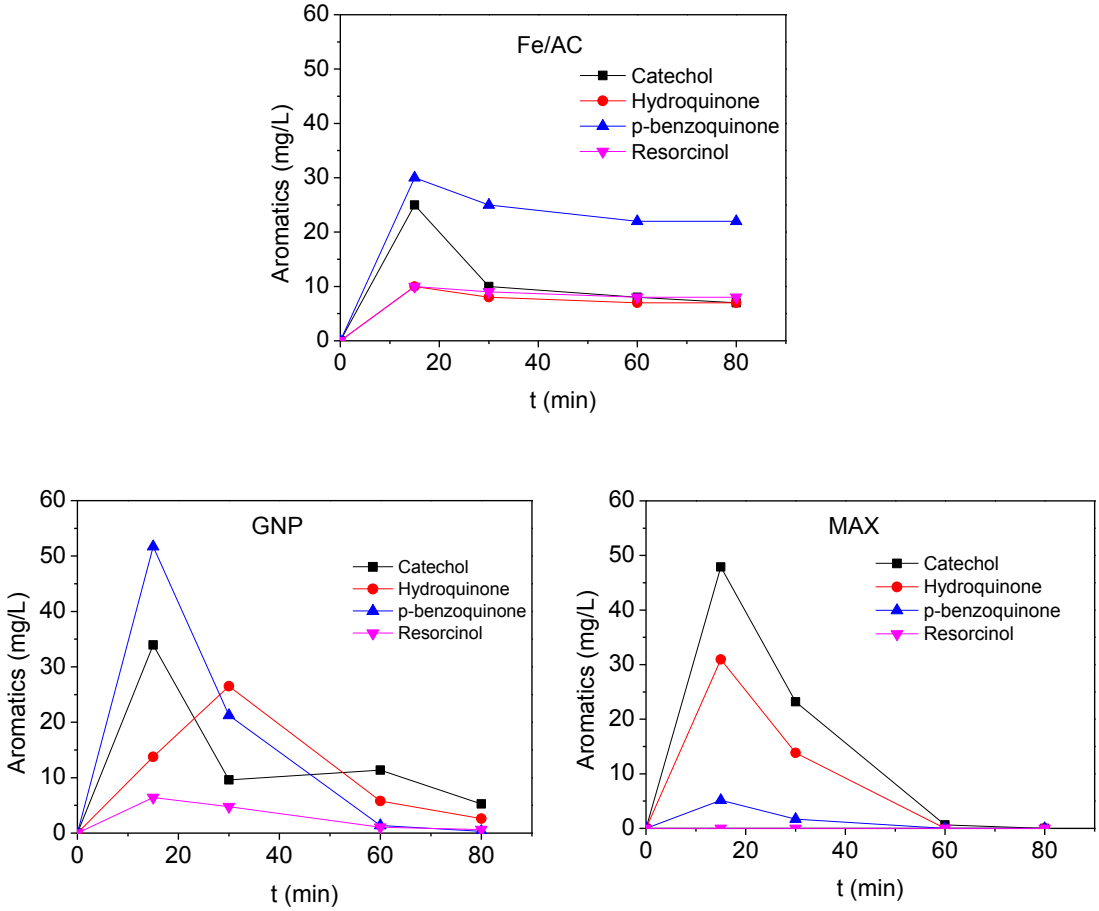

Figure S2. Continuous evolution of aromatic concentration in the CWPO with Fe/AC, GNP and MAX catalysts

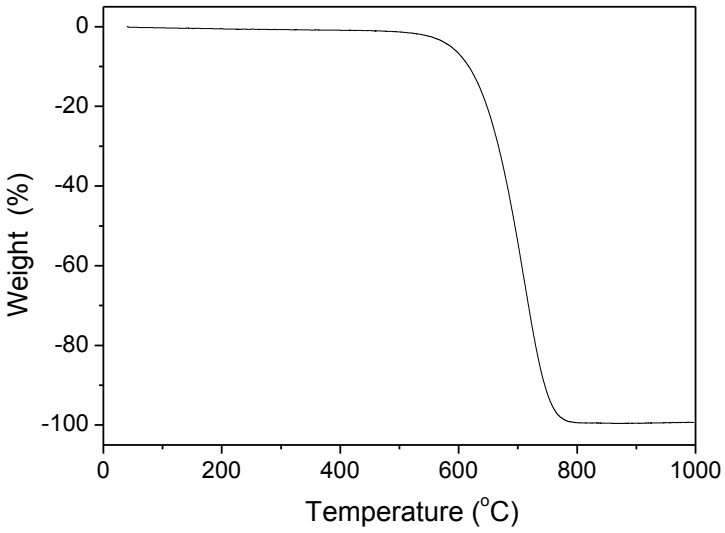

Figure S3. Thermogravimetric analysis of the GNP catalyst

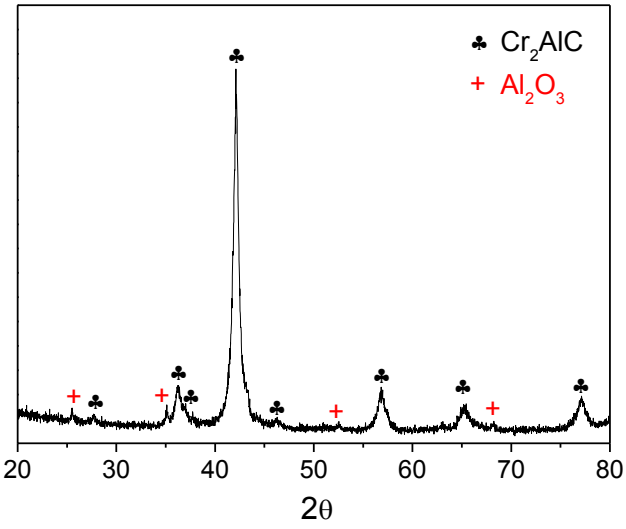

Fig. S4. X-ray diffraction (XRD) spectra of Cr_2AlC MAX catalyst

***Declaration of Interest Statement**

Declaration of interests

☒ The authors declare that they have no known competing financial interests or personal relationships that could have appeared to influence the work reported in this paper.

☐The authors declare the following financial interests/personal relationships which may be considered as potential competing interests:

Author Contributions Section:

J. Carbajo: Conceptualization, Methodology, Formal analysis, Investigation, Writing - Original Draft

A. Quintanilla: Conceptualization, Writing - Review & Editing, Supervision

A. L. Garcia-Costa: Methodology, Investigation, Writing - Review & Editing

J. González-Julián: Conceptualization, Methodology, Investigation

M. Belmonte. Methodology, Resources

P. Miranzo: Methodology, Resources

M. I. Osendi: Methodology, Resources

J. A. Casas: Conceptualization, Project administration, Funding acquisition, Supervision